

Experimental Investigation of the Electrical Wiring Configuration of the HK40 Hall Thruster Operation

Ugur Kokal¹ , Nazli Turan¹ , Murat Celik¹ 

¹. Boğaziçi University  – Department of Mechanical Engineering – Istanbul – Türkiye.

*Correspondence author: murat.celik@boun.edu.tr

ABSTRACT

Vacuum chambers providing a low pressure environment similar to the vacuum environment in low earth orbit have been used for the testing of plasma thrusters. A significant proportion of research on the effects of vacuum facility on plasma thrusters has focused on the effects of background pressure and plume expansion; however, the electrical interaction of the conductive chamber walls with the plasma thrusters needs to be explored further. In this study, the operation of a prototype Hall thruster, HK40, was investigated to understand the effects of wiring configuration of the thruster-cathode-chamber system. During the tests, the thruster was operated in two different grounding configurations. A resistance analogy regarding the changes in the electrical potentials and measured currents was introduced. The calculated thrust and efficiency values of the two configurations were compared. This study shows that the current extracted from the emitter surface of the cathode, along with the cathode-to-ground voltage can be used to estimate the thrust and thruster efficiency. In addition, the theoretical predictions were compared with the values based on the measurements made with an in-house-built inverted pendulum type thrust stand. The presented results show that the thrust and efficiency values are predicted with 3.4% and 8.3% uncertainty, respectively.

Keywords: Electric propulsion; Hall thrusters; Vacuum chambers; Hollow cathodes.

INTRODUCTION

Space propulsion systems are used for propulsive needs of satellites in orbit or spacecraft for deep space missions (Martinez-Sanchez and Pollard 1998; Mazouffre 2016). While the chemical propulsion systems currently present the only viable solution for launch vehicles and are unquestionably more suitable for maneuvers that require fast burns due to their much higher thrust levels, electric propulsion systems can provide the same delta-V while consuming much less propellant compared to their chemical counterparts. Among electric propulsion concepts, Hall thrusters are the most employed type for commercial operations and earth-orbiting satellites (Frieman *et al.* 2016; Lev *et al.* 2019; Potrivitu *et al.* 2020; Huo 2022). As Hall thrusters gain flight heritage, they are also being increasingly considered for deep space missions (Brophy *et al.* 2012; Levchenko *et al.* 2018).

The characterization and lifetime testing of the electric propulsion systems are conducted inside vacuum chamber test facilities. These vacuum test facilities provide the vacuum environment similar to low earth orbit with the background pressure levels on the order of 10^{-5} Torr. Although, there are a vast number of studies concerning the effects of background pressure on thruster operation and

Received: July 01, 2023 | **Accepted:** Sept. 14, 2023

Section editor: José Atilio Fritz Fidel Rocco 

Peer Review History: Single Blind Peer Review.



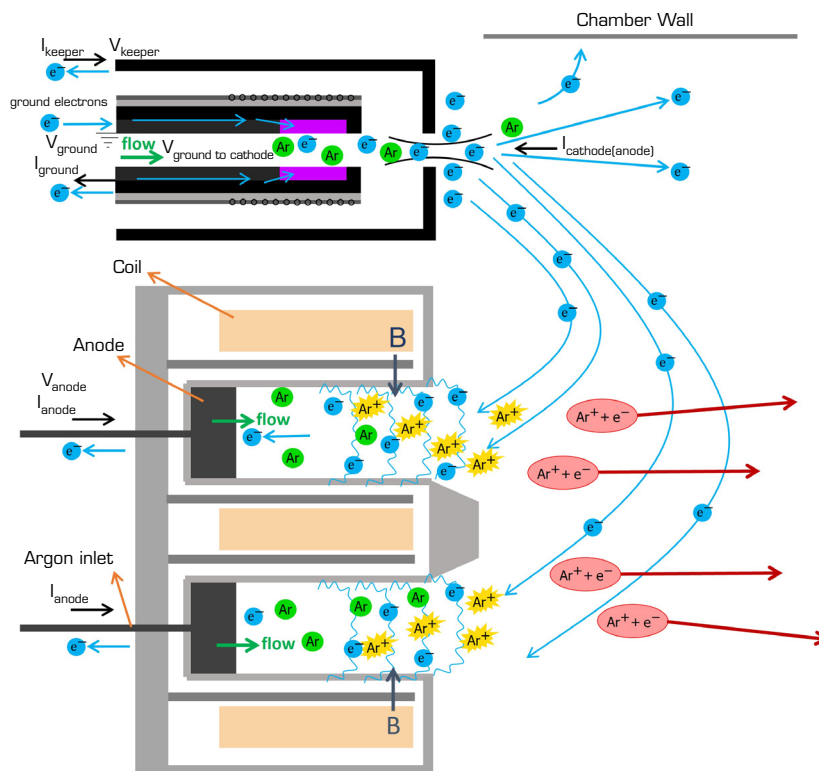
This is an open access article distributed under the terms of the Creative Commons license.

plume expansion (Diamant *et al.* 2014; Huang *et al.* 2014; Brown and Gallimore 2011; Nakles and Hargus Junior 2011; MacDonald-Tenenbaum *et al.* 2019; Ortega *et al.* 2020; Cichocki *et al.* 2020; Walker 2005), the possible electrical current interactions with the chamber walls and the effect of electrical wiring configuration need to be investigated further (Frieman *et al.* 2016, Walker *et al.* 2016a; Frieman *et al.* 2014). In laboratory experiments, the walls of the vacuum chamber are electrically grounded; however, this condition is not an accurate representation of the actual flight environment where no such electrical ground would be present. Furthermore, magnetic field topology and cathode position yield multifaceted interactions with the chamber walls (Walker *et al.* 2016a; Walker *et al.* 2016b).

Hall thrusters rely on externally applied electric and magnetic fields for the creation of plasma and for expelling the ions of this plasma at high velocities to generate thrust. Electrons are emitted by an external source, generally a hollow cathode, to start the plasma discharge inside the thruster discharge channel via electron impact ionization of the neutral propellant gas. The same electron source also provides electrons for the neutralization of the ion beam exiting the thruster. While the ions are axially accelerated by the applied electric field, the magnetic field causes the electrons to have a cycloid motion in the azimuthal direction due to their much lower mass. The electrons expelled from the cathode track the magnetic field lines from the cathode to the thruster. As the magnetic field topology are formed with electromagnets orienting electrons towards the inside of the discharge channel, they experience cyclotron motion with a frequency, $\omega_e = eB/m_e$. Cyclotron motion frequency of the electrons is higher than the frequency of the ions. Besides, cyclotron frequency of electrons is higher than their collisional frequency, ν_e , such that $\omega_e \gg \nu_e$ (Ahedo and Gallardo 2003). The $\mathbf{E} \times \mathbf{B}$ drift is generated in the discharge chamber and contributes to the Hall current in the region with the maximum magnetic flux density (Xu and Walker 2014). The Hall parameter, β , is defined by Eq. 1

$$\beta = \frac{\omega_e}{\nu_e} = \frac{eB}{m_e \nu_e} \quad (1)$$

where m_e and e are the electron mass and electron charge, respectively. Since the electrons are well magnetized, in $\mathbf{E} \times \mathbf{B}$ drift region, the Hall parameter has high values (Xu and Walker 2014). Figure 1 illustrates the paths of the electrons for a Hall thruster.



Source: Elaborated by the authors.

Figure 1. Schematic of the electron paths in a Hall thruster cathode system inside a vacuum chamber.

For Hall thrusters, the Hall parameter is large for the region where the magnetic flux density is high while the electrical resistivity is also high in these regions with the limited electron flow towards the anode in the channel. Furthermore, environments with different surface potentials or grounding/floating settings can alter the electron pathways resulting in a loss of the produced electrons. Since the magnetic field lines substantially affect the ionization and the extracted current from a discharge, the proper design of the magnetic field topology is crucial. The challenges in the design of the electrical and magnetic circuit of the thruster largely stem from the anomalous behavior of the electrons within the channels (Mikellides and Ortega 2019). While this behavior presents a complexity for the design and modelling of Hall thrusters, simplified assumptions can provide a way to estimate the thruster performance by macro-scale measurements that are readily made during tests, such as the measurements of voltages and currents.

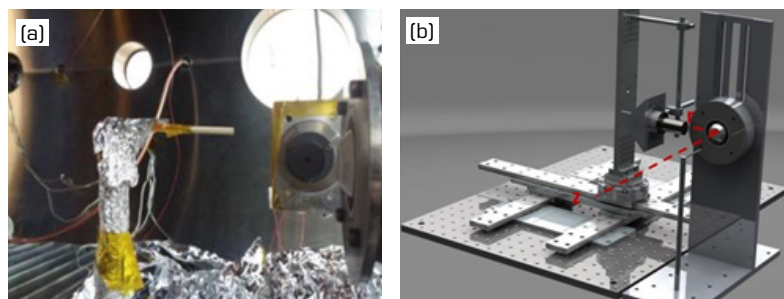
In this study, we aim to investigate the role of the chamber in estimating thruster efficiency by providing a comparison between the grounded and the floating electrical wiring configurations. The HK40, an experimental SPT type Hall effect thruster which was built at the Bogazici University Space Technologies Laboratory (BUSTLab), was used as the test bed for the investigation. A laboratory type LaB_6 cathode, also designed and developed at BUSTLab, was used as the cathode for the operation of this thruster (Kurt *et al.* 2017). The details of the test setup and the equipment are discussed in the following section.

EXPERIMENTAL SETUP

BUSTLab vacuum facility (Korkmaz 2015) is used for the experiments. The vacuum chamber has a diameter of 1.5 m and a length of 2.7 m. Vacuum level on the order of 3×10^{-6} Torr is reached with the use of two 12 inch cryopumps without any gas flow to the chamber. As the propellant, argon was supplied to the thruster (18 sccm) and to the cathode (2.2 sccm) through the chamber ports and controlled by a set of MKS flow controllers. For this rate of propellant flow to the thruster and cathode, the pressure of the chamber was measured to be 4.2×10^{-5} Torr during the tests. A Sorensen DCS600-1.7 was utilized for powering the cathode and a Glassman FL1250F1.2 power source was used for the thruster.

HK40 Hall Effect Thruster

HK40 is a prototype Hall thruster that utilizes a dielectric discharge chamber with outer diameter of 40 mm (Turan 2016). The thruster employs five identical cylindrical electromagnets, each with a diameter of 1/2 inch and a length of 1 inch long cylindrical electromagnets; one of these electromagnets are placed inside the coaxial channel and the remaining four are on the outside. A side view picture along with a rendering of the CAD drawing of the HK40 Hall thruster with the LaB_6 hollow cathode are shown in Fig. 2.



Source: Elaborated by the authors.

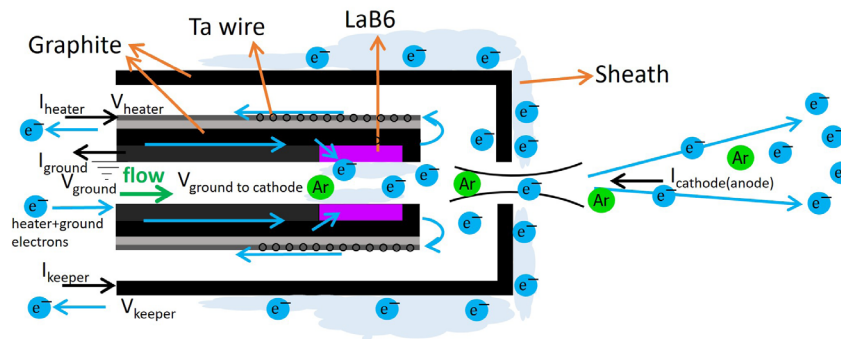
Figure 2. (a) HK40 Hall thruster and the LaB_6 hollow cathode with the Langmuir probe (b) Illustration of the test assembly with the vacuum translational stage (dashed lines indicating the axial and radial directions).

BUSTLab Hollow Cathode

The hollow cathode used for the operation of the HK40 Hall thruster utilizes a LaB_6 tube with an inner diameter of 2 mm, outer diameter of 4 mm and length of 10 mm as the thermionic emission material. The cathode tube of this hollow cathode is made of graphite with an outer diameter of 6 mm and length of 48 mm. This cathode has a unique heater assembly: tantalum wire of 0.25 mm diameter is wrapped around a shapal ceramic tube with external grooves of helical geometry. For electrical connection

of the heater circuit, the tantalum wire is continued to wrap around the grooves on a graphite part that is placed coaxially over the cathode tube (Kurt *et al.* 2017; Kokal *et al.* 2021).

The LaB_6 insert placed in the cathode tube is the source of electrons leaving the cathode. The insert is at ground potential as seen in Fig. 3. As the LaB_6 insert starts emitting electrons, it will start attracting electrons from the ground since it is momentarily electron deficient. As discussed in the next section, during the experiments, cathode current, which is generated by the electrons extracted from the ground, is measured.



Source: Elaborated by the authors.

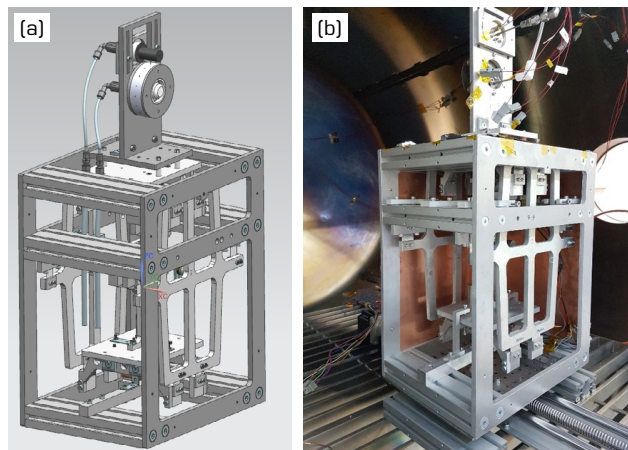
Figure 3. Schematic of electron extraction from LaB_6 cathode.

Langmuir Probe

A single Langmuir probe is used to measure the electron temperature and plasma potential of the thruster plume plasma. This Langmuir probe employs a molybdenum rod with a diameter of 1 mm placed inside a single hole, 3.18 mm outer diameter alumina tube (Yildiz and Celik 2019). For biasing the probe electrode and measuring the current collected by the electrode, a Keithley 2410 sourcemeter is used.

Thrust Stand

The thrust stand, built in-house at BUSTLab, utilizes an inverted pendulum mechanism (Kokal and Celik 2017; Kokal 2018) with two horizontal platforms and two pendulum arms. Counterweights are utilized to balance the weight of the thruster, as a result the effect of the thruster weight on thrust measurements is mitigated. The pendulum mechanism is assembled with stainless steel flexures. Thrust stand has a measurement accuracy of ± 0.3 mN. The thrust measurements of the HK40 Hall thruster were performed for various operation conditions (see Fig. 4 for the configuration).

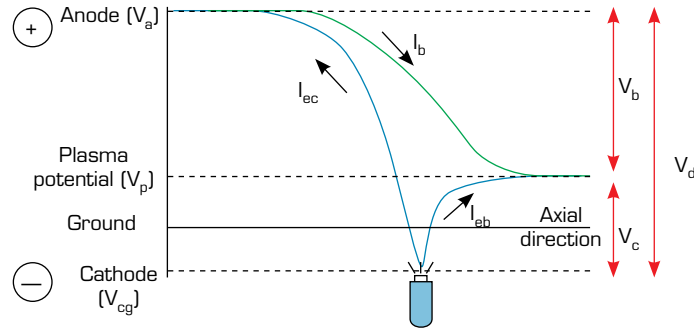


Source: Elaborated by the authors.

Figure 4. HK40 Hall thruster on the thrust stand.

COMPARISON OF TWO DIFFERENT WIRING CONFIGURATIONS

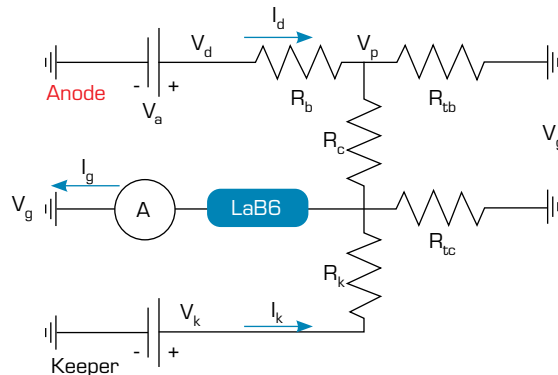
We introduce a circuit analogy that contains potentials and currents in the thruster-cathode-chamber system. The resistances are defined between the potentials, which are represented in the voltage schematic as in Fig. 5. The discharge potential (V_d) is the difference between the anode potential (V_a) and the cathode potential (V_{cg}). The plasma potential (V_p) is the voltage level that is experimentally determined in the plume region, where ion acceleration is finalized. The ions are accelerated with the beam potential (V_b), which is the voltage difference between the anode and plasma voltages. The cathode coupling potential (V_c) is the difference of the plasma and the cathode potential.



Source: Elaborated by the authors.

Figure 5. Hall thruster voltage schematic with corresponding currents.

Two representative schematics are introduced to illustrate the thruster-cathode-chamber system electrical circuits for laboratory and in-flight conditions. In the *grounded setup*, the power supplies, which provide the anode and keeper voltages, are grounded to the vacuum chamber (V_g). A multimeter is placed between the cathode and the ground in order to measure the cathode to ground current (I_g). In this setup, the cathode voltage (V_{cg}) is zero, therefore the anode voltage (V_a) and the discharge voltage (V_d) are equal. The value of the discharge voltage is read from the power supply. Figure 6 shows the defined potentials with resistances and currents for the *grounded setup*.

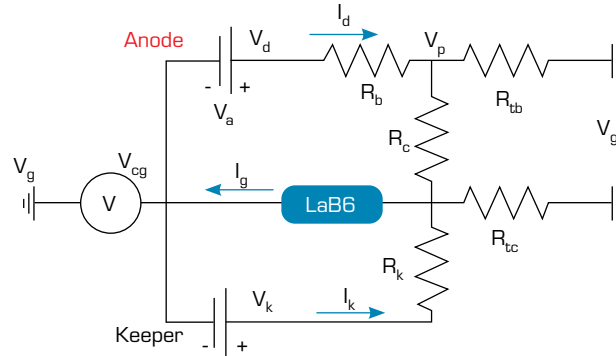


Source: Elaborated by the authors.

Figure 6. Schematic of the grounded setup electrical configuration of thruster-cathode system.

The anode and cathode form a closed circuit where R_b is the resistance between plasma and anode, R_c is the resistance between plasma and cathode (LaB_6 insert) and R_k is the resistance between keeper and cathode (LaB_6 insert). Here, the magnetic field topology in the discharge channel determines R_b and it is proportional to the square of the Hall parameter as in Eq. 1. Hence, the increased strength of the magnetic field increases R_b . The cathode placement, as well as the topology of the external magnetic field, determines R_c . The resistance inside the hollow cathode between the keeper electrode and the LaB_6 insert material is represented by R_k . As the experiments are conducted in the vacuum chamber, the resistance between the thruster plume and vacuum chamber wall, R_{tb} , and the resistance between the cathode and the vacuum chamber wall, R_{tc} , are added to the system.

In the floating configuration, as depicted in Fig. 7, the negative leads of the anode and keeper power supplies, and the negative lead of the cathode heater circuit are all connected at a floating common point (*floating ground*). The negative lead of the cathode heater circuit completes the circuit through the cathode insert material. A multimeter placed between the ground of the vacuum chamber and the floating ground is used to measure the voltage V_{cg} between the floating common ground voltage and the ground voltage (the ground of the vacuum chamber and hence the Earth). In the floating configuration, the cathode voltage V_{cg} is not zero, therefore the discharge voltage is equal to the difference between the anode voltage V_a and the cathode voltage (V_{cg}). This setup better resembles the electrical circuit of a thruster on a satellite, where the components of the system are powered with respect to V_{cg} instead of Earth's ground.



Source: Elaborated by the authors.

Figure 7. Schematic of the floating setup electrical configuration of the thruster-cathode system.

ESTIMATION OF THRUST AND EFFICIENCY

The efficiency and thrust of the thruster are estimated with the help of the introduced circuit analogy using readily measurable voltage and current values as well as the Langmuir probe measurements. In this section, thrust and efficiency calculations are presented. For the grounded setup, the measured current between the LaB_6 insert and the ground as depicted in Fig. 6 is used. Similarly, for the floating setup, the measured voltage between the floating common ground and the ground as depicted in Fig. 7 is used.

As stated earlier, tests are conducted with argon as the propellant with an anode propellant flow rate of 18 sccm and cathode propellant flow rate of 2.2 sccm. For the calculations, singly ionized argon ions are assumed. The fraction of the propellant leaving the thruster as ions, namely the current efficiency, η_p , was estimated to be in the range of 75-80% (Ross and King 2007). The divergence half angle was taken to be 37 degrees (Turan 2016; Baird *et al.* 2021). The beam divergence efficiency, η_{dp} value was obtained from the cosine of this angle.

Calculating efficiency from the ground current

The ions are created inside the discharge channel and then accelerated towards the downstream plume region from the location where they are created. The electric potential in the plume plasma is affected by the topology of the magnetic field, the electron current supplied from the cathode, the cathode position, and the characteristics of the discharge. Despite the electric potential of the region in the discharge channel where the ions are created slightly lower than the electric potential of the anode, the beam power can be estimated by Eq. 2:

$$P_b = I_b(V_a - V_p) = I_b(V_d - V_p) = I_b V_b \quad (2)$$

where the plasma potential, V_p , is measured with a Langmuir probe.

The beam current (I_b), that is the current due to the expelled ions, is the difference between the discharge current (I_d) and the portion of the cathode electron current backstreaming towards the anode (I_{ec}) (Goebel and Katz 2008). The discharge current is generated by the backstreaming electrons from the cathode and also by the ionization of the neutrals (Eq. 3):

$$I_d = I_{ec} + I_b \quad (3)$$

Where I_{ec} , the backstreaming cathode electrons, is measured from the current drawn from the ground (see Fig. 6). One should also note that the same amount of electrons and ions are generated in the plasma discharge due to ionization (Eq. 4):

$$I_b = I_{ei} \quad (4)$$

where I_{ei} is the electron current due to ionization. The created ions are ejected towards the exit. Electrons move towards the anode as shown in Fig. 1. Thrust in more general terms is defined by Eq. 5:

$$T = \dot{m}_i v_{avg} \quad (5)$$

where $\dot{m}_i = n_i \dot{m}$ is the propellant mass flow rate that is ionized, n_i is the ionization efficiency, and v_{avg} is the mean value of exit velocity of ions in axial direction given by Eq. 6:

$$v_{avg} = \sqrt{n_d \frac{2e(V_d - V_p)}{M_i}} \quad (6)$$

where M_i is the mass of an ion, n_d is the beam divergence coefficient and e is the electron charge (Sommerville and King 2007). The thrust is calculated by Eq. 7:

$$T = \frac{I_b M_i}{e} \sqrt{n_d \frac{2e(V_d - V_p)}{M_i}} \quad (7)$$

The efficiency is evaluated using Eq. 8:

$$\eta_{anode} = \frac{n_i n_d \dot{m}_i e (V_d - V_p)}{M_i P_{anode}} \quad (8)$$

where \dot{m}_i is the ion mass flow rate and $P_{anode} = I_d V_d$ is the total anode power.

Calculating efficiency from cathode to ground voltage

For the floating setup, as seen in Fig. 7, the cathode to ground voltage, V_{cg} , which is the cathode voltage, is measured. For this configuration, the discharge current (I_d) will again be the total of the beam current (I_b) and the current due to the backstreaming electrons, I_{ec} .

As discussed earlier, a majority of the electrons leave the cathode exit into the far-field plume for the neutralization of the beam ions. The remainder of the electrons backstream towards the anode causing the ionization of the neutral propellant released from the anode region. In order to fully resolve this electron current transport, a fast, spatial sweeping probe is needed, yet it is experimentally challenging. Thus, based on the studies in the literature (McDonald and Gallimore 2011; Smith and Cappelli 2010), the percentage of the backstreaming electrons was taken to be on the order of 20% of the discharge current.

The electric potential that causes the acceleration of the ions is the difference between the plasma voltage and applied anode voltage as shown in Fig. 5. Since the discharge voltage is with respect to the floating ground, the cathode to ground voltage is also needed to be added to the discharge voltage to obtain the anode voltage (Eq. 9).

$$V_b = V_d + V_{cg} - V_p \quad (9)$$

The thrust is calculated by Eq. 10:

$$T = \frac{I_b M_i}{e} \sqrt{n_d \frac{2e(V_d + V_{cg} - V_p)}{M_i}} \quad (10)$$

Hence the thrust efficiency is:

$$\eta_{anode} = \frac{n_i n_d \dot{m}_i e (V_d + V_{cg} - V_p)}{M_i P_{anode}} \quad (11)$$

where $I_d V_d$ is the total anode power, P_{anode} .

RESULTS AND DISCUSSIONS

As described earlier, the thruster magnetic field is created by four outer coils and one inner coil. For Hall thrusters, a high Hall parameter, β , with a high magnetic field B results in an increase in the beam resistance (R_b) in the acceleration region. Therefore, the potential difference between the cathode and the anode is concentrated in the acceleration region. In the experiments, for both configurations, the thruster is operated at discharge voltage of 200V and discharge current of 1.2A. For these conditions, the calculated efficiency and thrust values are presented in Table 1.

Table 1. Detailed comparison of calculated values of HK40 Hall thruster for grounded and floating wiring configurations.

Parameter	Grounded	Floating
Plasma Potential, V_p	25 V	26 V
Cathode Voltage, V_{cg}	0 V	-27 V
Backstreaming Current, I_{bc}	0.4 A	0.24 A*
Thrust, T	8.2 mN	9.0 mN
Efficiency, η_{anode}	0.21	0.26

*The backstreaming electron current fraction is taken to be 20% of the total discharge current (McDonald and Gallimore 2011).
Source: Elaborated by the authors.

For the grounded setup, the efficiency and thrust values were calculated using Eqs. 7 and 8. For this setup, as described earlier, the power supplies were grounded, and the current drawn from the ground was measured using a multimeter serially connected between the return wire of the heater circuit and the ground. The plasma potential in the plume region was measured using a single Langmuir probe.

For the floating setup tests, the thrust was calculated using Eq. 10 by measuring the cathode to ground voltage and the efficiency was calculated using Eq. 11. During the floating setup experiments, all the power supplies were connected to a common ground as depicted in Fig. 7. When the calculated values are compared, it is observed that the floating setup yielded higher predicted thrust and efficiency values compared to the grounded setup as seen in Table 1.

For the floating setup, thrust measurements were conducted with the in-house built thrust stand. As seen in Table 2, the calculated and measured values showed differences for both thrust and efficiency. Although the floating setup better represents satellite operation in space, vacuum chamber walls affect the electron pathways during the tests. In the floating setup, the cathode has a negative voltage, thus the chamber walls attract a portion of the electrons. However, in the grounded setup, cathode voltage is kept at ground voltage of the vacuum tank walls, therefore electron current from the cathode to the chamber walls is expected to be smaller, which may present a better representation of space conditions, as in space conditions electron pathways through R_{tb} and R_{tc} resistances do not exist (see Fig. 7). This is also a loss mechanism as the electrons generated inside the cathode are wasted without being efficiently utilized for ionization or neutralization purposes. This is one plausible explanation for why the measured thrust is lower than the calculated value. One also must note that there is a ± 0.3 mN uncertainty in thrust measurements. In addition, some of the assumptions such as the beam divergence angle can result in an over-estimation for the calculated thrust values.

Table 2. Comparison of calculated and measured values of HK40 Hall thruster for floating wiring configuration.

Parameter	Calculated	Measured
Thrust, T	9.0 mN	8.7 ± 0.3 mN
Efficiency, η_{anode}	0.26	0.24 ± 0.01

Source: Elaborated by the authors.

Due to the decrease in the magnetic field intensity away from the thruster, the current pathways for the electrons may change towards the thruster body for the region near to the discharge channel exit or towards the vacuum chamber walls for the regions away from the thruster. As a result of such electron recombination pathways, different efficiency and thrust values can be obtained for the ground and in space operations as observed in this study.

CONCLUSIONS

This study presents the investigation of the effects of wiring configuration of the thruster-cathode-chamber system using two different grounding configurations on the operational characteristics of a prototype Hall thruster, HK40. Without considering the inherently complex electron pathways, we provided a macro-scale resistance analogy regarding the changes in the electrical potentials and measured currents to interpret thruster performance. The thrust and efficiency of the thruster were estimated with the help of the introduced circuit analogy using readily measurable voltage and current values as well as the Langmuir probe measurements. The theoretical predictions were also compared with the thrust stand measurements for the floating configuration since it presents a comparison with space operation. We estimated the thrust and efficiency with 3.4% and 8.3% uncertainty, respectively while operating the thruster at 200V of discharge voltage and 1.2A of discharge current. Our representative method can help understand the electron pathways through resistances, since we already measure voltages and currents during tests. Future work would be operating the thruster in a wider range to validate its operation and reducing the number of assumptions in our calculations after integrating plume angle measurements with a Faraday probe.

CONFLICT OF INTEREST

Nothing to declare.

AUTHOR CONTRIBUTIONS

Conceptualization: Turan N and Kokal U; **Data curation:** Turan N and Kokal U; **Formal analysis:** Turan N and Kokal U; **Acquisition of funding:** Celik M; **Research:** Turan N, Kokal U and Celik M; **Methodology:** Turan N, Kokal U and Celik M; **Project administration:** Celik M; **Supervision:** Celik M; **Validation:** Turan N and Kokal U; **Visualization:** Turan N and Kokal U; **Writing - Preparation of original draft:** Celik M, Kokal U and Turan N; **Writing - Proofreading and editing:** Celik M, Kokal U and Turan N.

FUNDING

Scientific and Technological Research Council of Turkey, <https://doi.org/10.13039/501100004410>.
Grant No: 214M572

ACKNOWLEDGMENTS

The authors would like to thank Professor Huseyin Kurt of Istanbul Medeniyet University for his contributions to the experimental setup and tests.

REFERENCES

- Ahedo E, Gallardo JM (2003) Scaling down Hall Thrusters. Paper presented at 28th Electric Propulsion Conference. IEPC; Toulouse, France.
- Baird M, Kerber T, McGee-Sinclair R, Lemmer K (2021) Plume Divergence and Discharge Oscillations of an Accessible Low-Power Hall Effect Thruster. *Appl Sci* 11(4):1973. <https://doi.org/10.3390/app11041973>
- Brophy JR, Friedman L, Culick F (2012) Asteroid Retrieval Feasibility. Paper presented at 2012 IEEE Aerospace Conference. IEEE; Big Sky, United States. <https://doi.org/10.1109/AERO.2012.6187031>
- Brown DL, Gallimore AD (2011) Evaluation of Facility Effects on Ion Migration in a Hall Thruster Plume. *J Propuls Power* 27(3):573-585. <https://doi.org/10.2514/1.B34068>
- Cichocki F, Merino M, Ahedo E (2020) Three-Dimensional Geomagnetic Field Effects on a Plasma Thruster Plume Expansion. *Acta Astronautica* 175:190-203. <https://doi.org/10.1016/j.actaastro.2020.05.019>
- Diamant KD, Liang R, Corey RL (2014) The Effect of Background Pressure on SPT-100 Hall Thruster Performance. Paper presented at 50th AIAA/ASME/SAE/ASEE Joint Propulsion Conference. AIAA; Cleveland, United States. <https://doi.org/10.2514/6.2014-3710>
- Frieman JD, King ST, Walker MLR, Khayms V, King D (2014) Role of a Conducting Vacuum Chamber in the Hall Effect Thruster Electrical Circuit. *J Propuls Power* 30(6):1471-1479. <https://doi.org/10.2514/1.B35308>
- Frieman JD, Walker JA, Walker MLR, Khayms V, King DQ (2016) Electrical Facility Effects on Hall Thruster Cathode Coupling: Performance and Plume Properties. *J Propuls Power* 32(1):251-264. <https://doi.org/10.2514/1.B35683>
- Goebel DM, Katz I (2008) *Fundamentals of Electric Propulsion: Ion and Hall Thrusters*. Hoboken: John Wiley & Sons. <https://doi.org/10.1002/9780470436448>
- Huang W, Kamhawi H, Lobbia RB, Brown DL (2014) Effect of Background Pressure on the Plasma Oscillation Characteristics of the HiVHAc Hall Thruster. Paper presented at 50th AIAA/ASME/SAE/ASEE Joint Propulsion Conference. AIAA; Cleveland, United States. <https://doi.org/10.2514/6.2014-3708>
- Huo Y (2022) Space Broadband Access: The Race Has Just Begun. *Computer* 55(7):38-45. <https://doi.org/10.1109/MC.2022.3160472>
- Kokal U (2018) Development of a Mili-Newton Level Thrust Stand for Thrust Measurements of Electric Propulsion Systems and UK90 Hall Effect Thruster (MS thesis). Istanbul: Bogazici University.
- Kokal U, Celik M (2017) Development of a Mili-Newton Level Thrust Stand for Thrust Measurements of Electric Propulsion Systems. Paper presented at 2017 8th International Conference on Recent Advances in Space Technologies (RAST). IEEE; Istanbul, Turkey. <https://doi.org/10.1109/RAST.2017.8002970>
- Kokal U, Turan N, Celik M (2021) Thermal Analysis and Testing of Different Designs of LaB6 Hollow Cathodes to be Used in Electric Propulsion Applications. *Aerospace* 8(8):215. <https://doi.org/10.3390/aerospace8080215>

- Korkmaz O, Jahanbakhsh S, Celik M, Kurt H (2015) Space Propulsion Research Vacuum Facility of the Bogazici University Space Technologies Laboratory. Paper presented at 2015 7th International Conference on Recent Advances in Space Technologies (RAST). IEEE; Istanbul, Turkiye. <https://doi.org/10.1109/RAST.2015.7208420>
- Kurt H, Kokal U, Turan N, Celik M (2017) Note: Coaxial-Heater Hollow Cathode. *Rev Sci Instrum* 88(6):066103. <https://doi.org/10.1063/1.4986111>
- Lev D, Myers RM, Lemmer KM, Kolbeck J, Koizumi H, Polzin K (2019) The Technological and Commercial Expansion of Electric Propulsion. *Acta Astronautica* 159:213-227. <https://doi.org/10.1016/j.actaastro.2019.03.058>
- Levchenko I, Xu S, Teel G, Mariotti D, Walker MLR, Keidar M (2018) Recent Progress and Perspectives of Space Electric Propulsion Systems Based on Smart Nanomaterials. *Nat Commun* 9(1):879. <https://doi.org/10.1038/s41467-017-02269-7>
- MacDonald-Tenenbaum N, Pratt Q, Nakles M, Pilgram N, Holmes M, Hargus Junior W (2019) Background Pressure Effects on Ion Velocity Distributions in an SPT-100 Hall Thruster. *J Propuls Power* 35(2):403-412. <https://doi.org/10.2514/1.B37133>
- Martinez-Sanchez M, Pollard JE (1998) Spacecraft Electric Propulsion-An Overview. *J Propuls Power* 14(5):688-699. <https://doi.org/10.2514/2.5331>
- Mazouffre S (2016) Electric Propulsion for Satellites and Spacecraft: Established Technologies and Novel Approaches. *Plasma Sources Sci Technol* 25(3):033002. <https://doi.org/10.1088/0963-0252/25/3/033002>
- McDonald MS, Gallimore AD (2011) Electron Trajectory Simulation in Experimental Hall Thruster Fields. Paper presented at 32nd International Electric Propulsion Conference. IEPC; Wiesbaden, Germany. [accessed 2023 Jan. 12]. <https://pepl.engin.umich.edu/pdf/IEPC-2011-243.pdf>
- Mikellides IG, Ortega AL (2019) Challenges in the Development and Verification of First-Principles Models in Hall-Effect Thruster Simulations that are Based on Anomalous Resistivity and Generalized Ohm's Law. *Plasma Sources Sci Technol* 28(1): 014003. <https://doi.org/10.1088/1361-6595/aae63b>
- Nakles MR, Hargus Junior WA (2011) Background Pressure Effects on Ion Velocity Distribution within a Medium-Power Hall Thruster. *J Propuls Power* 27(4):737-743. <https://doi.org/10.2514/1.48027>
- Ortega AL, Mikellides IG, Chaplin VH, Snyder JS, Lenguito G (2020) Facility Pressure Effects on a Hall Thruster with an External Cathode: I. Numerical Simulations *Plasma Sources Sci Technol* 29(3):035011. <https://doi.org/10.1088/1361-6595/ab6c7e>
- Potrivitu G-C, Sun Y, Rohaizat MWA, Cherkun O, Xu L, Huang S, Xu S (2020) A Review of Low-Power Electric Propulsion Research at the Space Propulsion Centre Singapore. *Aerospace* 7(6):67. <https://doi.org/10.3390/aerospace7060067>
- Ross JL, King LB (2007) Energy Efficiency in Low Voltage Hall Thrusters. Paper presented at 43rd AIAA/ASME/SAE/ASEE Joint Propulsion Conference & Exhibit. AIAA; Cincinnati, United States. <https://doi.org/10.2514/6.2007-5179>
- Smith AW, Cappelli MA (2010) Single Particle Simulations of Electron Transport in the Near-Field of Hall Thrusters. *J Phys D: Appl Phys* 43(4):045203. <https://doi.org/10.1088/0022-3727/43/4/045203>
- Sommerville JD, King LB (2007) Effect of Cathode Position on Hall-Effect Thruster Performance and Cathode Coupling Voltage. Paper presented at 43rd AIAA/ASME/SAE/ASEE Joint Propulsion Conference & Exhibit, AIAA; Cincinnati, United States. <https://doi.org/10.2514/6.2007-5174>
- Turan N (2016) Experimental Investigation of the Effects of Cathode Position on HK40 Hall Effect Thruster Performance and Cathode Coupling (PhD thesis). Istanbul: Bogazici University.

Walker JA, Frieman JD, Walker MLR, Khayms V, King D, Peterson PY (2016a) Electrical Facility Effects on Hall-Effect-Thruster Cathode Coupling: Discharge Oscillations and Facility Coupling. *J Propuls Power* 32(4):844-855. <https://doi.org/10.2514/1.B35835>

Walker JA, Langendorf SJ, Walker MLR, Khayms V, King D, Peterson P (2016b) Electrical Facility Effects on Hall Current Thrusters: Electron Termination Pathway Manipulation. *J Propuls Power* 32(6):1365-1377. <https://doi.org/10.2514/1.B35904>

Walker MLR (2005) Effects of Facility Backpressure on the Performance and Plume of a Hall Thruster (master's thesis). Ann Arbor: University of Michigan.

Xu KG, Walker MLR (2014) Effect of External Cathode Azimuthal Position on Hall-Effect Thruster Plume and Diagnostics. *J Propuls Power* 30(2):506-513. <https://doi.org/10.2514/1.B34980>

Yildiz MS, Celik M (2019) Plume Diagnostics of BUSTLab Microwave Electrothermal Thruster using Langmuir and Faraday Probes. *Plasma Sci Technol* 21(4):045505. <https://doi.org/10.1088>